Title

Transcriptionally and Functionally Distinct Mesenchymal Subpopulations Are Generated from Human Pluripotent Stem Cells

Journal

Stem Cell Reports, 10(2)

ISSN

2213-6711

Authors

Chin, Chee Jia
Li, Suwen
Corselli, Mirko
et al.

Publication Date

2018-02-01

DOI

10.1016/j.stemcr.2017.12.005

Peer reviewed

Stem Cell Reports
Article

OPEN ACCESS

Transcriptionally and Functionally Distinct Mesenchymal Subpopulations Are Generated from Human Pluripotent Stem Cells

Chee Jia Chin,[1] Suwen Li,[1] Mirko Corselli,[2] David Casero,[1] Yuhua Zhu,[1] Chong Bin He,[1] Reef Hardy,[3,4,5,6] Bruno Péault,[1,3,4,5,7] and Gay M. Crooks[1,5,8,9,*]

[1]Department of Pathology and Laboratory Medicine, David Geffen School of Medicine (DGSOM), University of California (UCLA), Los Angeles, CA 90095, USA
[2]Becton Dickinson, San Diego, CA 92121, USA
[3]Department of Orthopedics, DGSOM, UCLA, Los Angeles, CA 90095, USA
[4]Orthopedic Hospital Research Center, UCLA, Los Angeles, CA 90095, USA
[5]Broad Stem Cell Research Center (BSCRC), UCLA, Los Angeles, CA 90095, USA
[6]Department of Medicine, University of Indiana, Indianapolis, IN 46202, USA
[7]Center for Regenerative Medicine, University of Edinburgh, Edinburgh EH16 4UU, UK
[8]Department of Pediatrics, DGSOM, UCLA, Los Angeles, CA 90095, USA
[9]Jonsson Comprehensive Cancer Center (JCCC), UCLA, Los Angeles, CA 90095, USA
*Correspondence: gcrooks@mednet.ucla.edu
https://doi.org/10.1016/j.stemcr.2017.12.005

SUMMARY

Various mesenchymal cell types have been identified as critical components of the hematopoietic stem/progenitor cell (HSPC) niche. Although several groups have described the generation of mesenchyme from human pluripotent stem cells (hPSCs), the capacity of such cells to support hematopoiesis has not been reported. Here, we demonstrate that distinct mesenchymal subpopulations co-emerge from mesoderm during hPSC differentiation. Despite co-expression of common mesenchymal markers (CD73, CD105, CD90, and PDGFRβ), a subset of cells defined as $CD146^{hi}CD73^{hi}$ expressed genes associated with the HSPC niche and supported the maintenance of functional HSPCs *ex vivo,* while $CD146^{lo}CD73^{lo}$ cells supported differentiation. Stromal support of HSPCs was contact dependent and mediated in part through high *JAG1* expression and low WNT signaling. Molecular profiling revealed significant transcriptional similarity between hPSC-derived $CD146^{++}$ and primary human $CD146^{++}$ perivascular cells. The derivation of functionally diverse types of mesenchyme from hPSCs opens potential avenues to model the HSPC niche and develop PSC-based therapies.

INTRODUCTION

Maintenance of *bona fide* self-renewing hematopoietic stem and progenitor cells (HSPCs) *ex vivo* remains challenging in part because of our limited ability to recapitulate the human HSPC niche in culture. Intensive research efforts have begun to uncover the cellular and molecular constituents of the niche that regulate self-renewal and differentiation of HSPCs. Through the use of knockout and transgenic mice, several cell populations have been described in terms of their spatial relationship to the bone and blood vessels of the bone marrow, and their differential expression of various markers and bioactive molecules (Ding et al., 2012; Itkin et al., 2016; Kobayashi et al., 2010; Kunisaki et al., 2013).

High expression of melanoma-associated cell adhesion molecule (CD146) identifies human pericytes, a cell type that ensheaths capillaries, venules, arterioles, and sinusoids (Crisan et al., 2008) and can establish a heterotopic hematopoietic stem cell (HSC) niche when transplanted into immunodeficient mice (Sacchetti et al., 2007). Unlike $CD146^{-}$ mesenchyme, monolayers of $CD146^{++}$ cells isolated from primary tissue (adult adipose tissue and fetal bone marrow) can support human HSPCs co-cultured for at least 2 weeks in the absence of exogenous cytokines (Corselli et al., 2013).

We and others have shown that mesenchymal cells can be differentiated from human pluripotent stem cells (hPSCs) (Chin et al., 2016; Ferrell et al., 2014; Hoffman and Calvi, 2014; Vodyanik et al., 2010). These previous studies identified mesenchyme as a single population defined mostly by expression of CD73 and/or CD105 and absence of hematopoietic and endothelial markers. We now report that the mesenchyme generated from hPSCs is functionally and transcriptionally heterogeneous. Our studies identified a distinct subpopulation of hPSC-derived mesenchyme that expressed high levels of CD146 and CD73 and low levels of PDGFRα (CD140a) and that was capable of supporting clonogenic, engraftable, and self-renewing human HSPCs *ex vivo* without exogenous cytokines. In contrast $CD146^{lo}CD73^{lo}$ mesenchyme showed significantly less capacity to support HSPCs. Transcriptome analysis revealed that the $CD146^{hi}CD73^{hi}$ cells expressed significantly higher levels than $CD146^{lo}CD73^{lo}$ cells of perivascular markers and niche factors known to have critical roles in HSC maintenance. HSPC support was dependent in part on cell-cell interactions and Notch signaling through stromal expression of JAG1, whereas

differentiation was promoted by WNT signaling. Closer transcriptional analysis, combining data from mesenchyme generated from hPSCs and human primary tissue, revealed that dominant pathways shared by the CD146^{++} populations were those related to vascular development, cell adhesion, and motility. Our data suggest that hPSC-derived mesoderm can generate mesenchymal cells phenotypically, functionally, and molecularly, similar to previously identified primary pericytes that contribute to the human HSPC niche.

RESULTS

Heterogeneity of Embryonic Mesoderm-Derived Mesenchymal Cells

We have previously characterized a human embryonic mesoderm progenitor (hEMP) population derived from hPSCs that marks the onset of mesoderm commitment and has the potential to generate a broad range of mesodermal derivatives, including mesenchyme, endothelium, and bone, three lineages that play a crucial role in the hematopoietic niche (Chin et al., 2016; Hoffman and Calvi, 2014). hEMPs were isolated at day 3.5 of mesoderm differentiation from H1 embryonic stem cells (Evseenko et al., 2010) (Figure 1A), and re-cultured using conditions that favor mesenchymal differentiation. After a further 14 days, cultures contained a mixture of CD31^{+}CD45^{-} endothelial cells and CD31^{-}CD45^{-} mesenchymal cells. The mesenchymal cells consisted of at least two populations that could be discriminated based on expression of CD146, CD73, and CD140a (PDGFRα) (Figure 1A). High co-expression of CD146 and CD73 identified a largely CD140a^{-} population, whereas CD146^{lo} cells expressed intermediate levels of CD73 and high levels of CD140a. This inverse expression pattern between CD146 and CD140a was consistent with mesenchyme derived from primary human lipoaspirates (Figure S1A). Despite the differential expression of CD146, CD73, and CD140a, both hPSC-derived mesenchymal subsets expressed classic mesenchymal markers CD90, CD105, CD44, and PDGFRβ (Figure S1B). Mesenchymal differentiation from two other hPSC lines, UCLA3 and UCLA6, yielded similar populations to the H1 line, with an inverse relationship of CD146 and CD73 to CD140a expression (Figures S2A and S2B). Although few CD146^{hi}CD73^{hi} cells were present early in differentiation (days 4–5), the inverse expression pattern of CD146 and CD73 to CD140a was present throughout mesenchymal differentiation (Figure S2C).

To better understand whether the phenotypes above identified distinct mesenchymal cell types, we focused our studies on cells that represented the extremes of these phenotypes: a CD146^{hi}CD73^{hi} population and a CD146^{lo}CD73^{lo} population (Figure 1A). Bromodeoxyuridine pulsing of hEMP-derived mesenchymal cultures showed that a significantly higher frequency of CD146^{hi}CD73^{hi} cells were cycling relative to CD146^{lo}CD73^{lo} cells (Figure 1B) ($p \leq 0.05$).

RNA sequencing (RNA-seq) profiling of the two mesenchymal populations demonstrated that 916 genes were differentially expressed (558 up- and 358 downregulated in CD146^{hi}CD73^{hi} relative to CD146^{lo}CD73^{lo} cells; false discovery rate [FDR] < 0.01) (Figure 1C). Across all hESC lines tested, CD146^{hi}CD73^{hi} mesenchyme expressed significantly higher levels of pericyte markers *CSPG4* (which encodes NG2), *NES* (NESTIN), *LEPR* (leptin receptor), and the β2-adrenergic receptor *ADRB2* (Crisan et al., 2008; Hoffman and Calvi, 2014; Kunisaki et al., 2013), and HSC regulatory genes, *KITLG*, *IGFBP2*, and *TNC* (Ding et al., 2012; Huynh et al., 2008; Nakamura-Ishizu et al., 2012; Zhang et al., 2008) (Figures 1C, S1C, S2A, and S2B). In contrast, the CD146^{lo}CD73^{lo} mesenchyme expressed significantly higher levels of the niche factors *CXCL12* and *ADRB3* (Greenbaum et al., 2013; Méndez-Ferrer et al., 2008) (Figure 1C). Expression of extracellular matrix genes was upregulated after the hEMP stage in both mesenchymal phenotypes (Figure 1C).

Mesenchymal Support of HSPCs *Ex Vivo*

The ability of hEMP-derived CD146^{hi}CD73^{hi} and CD146^{lo}CD73^{lo} cells to support HSPCs *ex vivo* was assessed by co-culturing cord blood (CB)-derived CD34^{+} cells on monolayers generated from each mesenchymal population. To determine the specific effect of each stromal subset, cultures were performed in basal medium with a low concentration of serum (5%) and without addition of cytokines.

Although total hematopoietic (CD45^{+} cells) output was similar with both mesenchymal populations (Figure 2A), co-cultures with CD146^{hi}CD73^{hi} cells retained a significantly higher frequency and number of total CD34^{+} cells than co-culture with CD146^{lo}CD73^{lo} mesenchymal cells (Figures 2B and 2C) ($p < 0.01$ and $p < 0.001$, respectively, $n = 16$). In particular, support of the more primitive CD34^{+}Lin^{-} subset was consistently seen in the CD146^{hi}CD73^{hi} co-cultures (Figure 2D). Myeloid output was higher in CD146^{hi}CD73^{hi} co-cultures, whereas more B lymphoid cells were generated on CD146^{lo}CD73^{lo} mesenchyme (Figures 2E and 2F). Significantly more clonogenic cells (colony-forming unit [CFU]-C) were maintained in CD146^{hi}CD73^{hi} co-cultures than CD146^{lo}CD73^{lo} co-cultures ($p < 0.001$, $n = 16$; Figure 2G). Of note, multiple other hPSC-derived phenotypic subsets were screened based on their CD146 and CD140a expression; irrespective

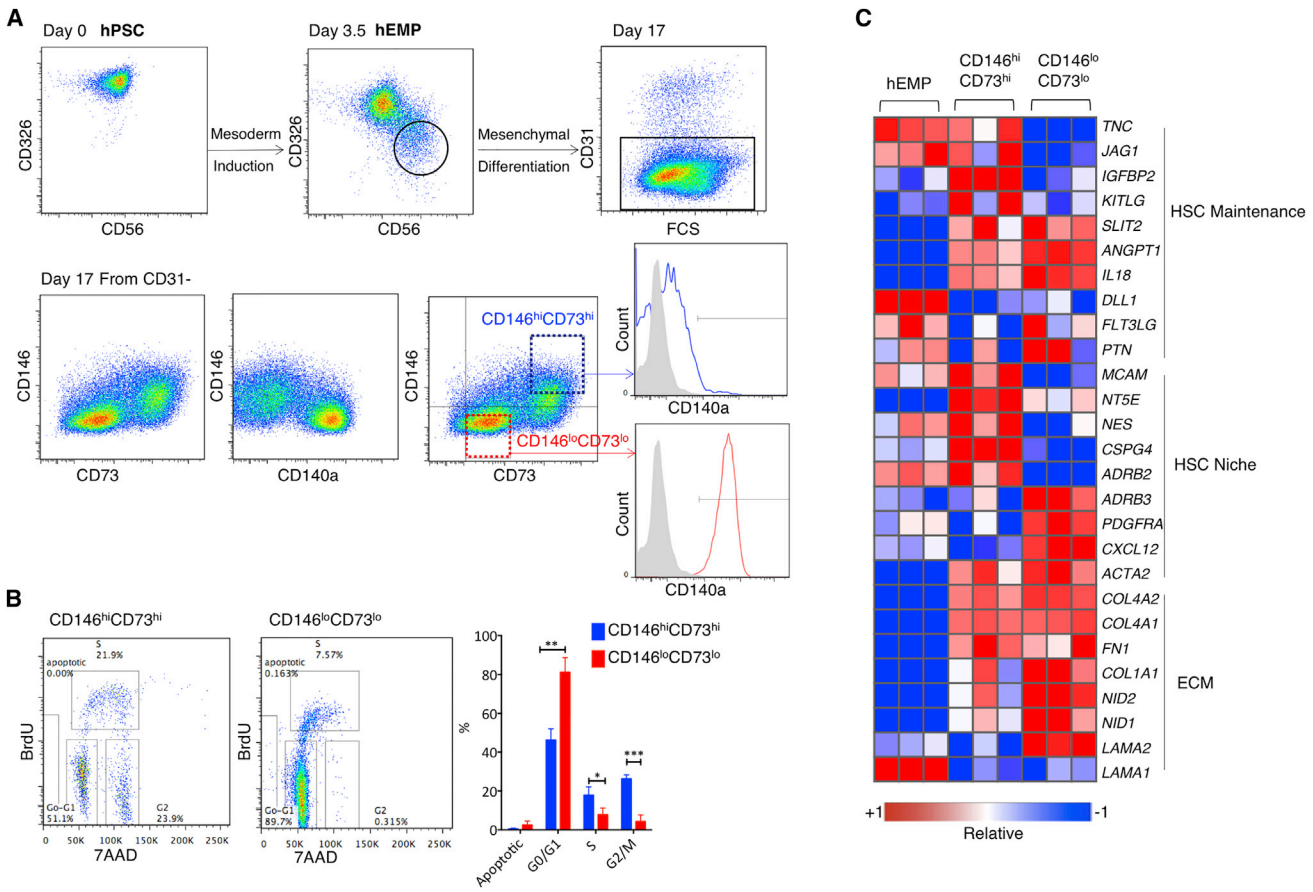

Figure 1. Immunophenotypic Fractionation of hPSC-Derived Mesenchyme Reveals Transcriptionally Distinct Populations

(A) hEMPs were generated from hPSC and isolated at day 3.5 by FACS for further differentiation in mesenchymal conditions. After 2 weeks, two distinct populations were identified within the CD31$^-$ (non-endothelial) cells, which were also CD45$^-$ (non-hematopoietic, not shown). CD146^{lo}CD73^{lo} cells (red) were CD140a$^+$, and CD146^{hi}CD73^{hi} cells (blue) were CD140^{lo} or CD140a$^-$ (representative data using H1 cells of n = 16 experiments).

(B) Cell-cycle analysis of hEMP-derived mesenchymal differentiation cultures at week 2, pulsed with bromodeoxyuridine (BrdU) for 40 min, and gated on CD31$^-$ mesenchyme, as shown in Figure 1A, as either "CD146^{hi}CD73^{hi}" or "CD146^{lo}CD73^{lo}." n = 3 biological replicates. The y axis shows the percentage of each mesenchymal phenotype in each stage of cell cycle, *p < 0.05, **p < 0.01, ***p < 0.001.

(C) Selected genes from RNA-seq profiling of hEMP, and hEMP-derived CD146^{hi}CD73^{hi} and CD146^{lo}CD73^{lo} mesenchyme (as in Figure 1A). Relative expression shown for each gene using its min/max moderate expression estimates as reference. n = 3 biological replicates. Error bars represent SEM. See also Figures S1 and S2.

of CD140a expression, those subsets with high levels of CD146 best supported HSPCs (Figure S3A).

When Lin$^-$CD34$^+$ CD38$^-$ cells, a more primitive HSC-enriched population were studied, the co-culture system was modified by adding exogenous growth factors to allow sufficient cell growth for analysis. In the presence of cytokines, both mesenchymal populations were able to support CD34$^+$ cells for 2–4 weeks. However, only the CD146^{hi}CD73^{hi} mesenchyme could maintain CD34$^+$CD38$^-$CD90$^+$CD45RA$^-$, phenotypic long-term HSCs (n = 4, p < 0.05), and CD34$^+$CD33$^-$ cells (Figure S3B), demonstrating again the functional differences between the two mesenchymal populations in HSPC support.

CD146^{hi}CD73^{hi} Mesenchyme Maintains Human HSPCs with Repopulating Ability and Self-Renewal Potential

To understand whether support of engraftable HSPCs was influenced by the different mesenchymal subsets, equal numbers of CD34$^+$ cells were co-cultured for 2 weeks with CD146^{hi}CD73^{hi} or CD146^{lo}CD73^{lo} cells, and then equal numbers of total hematopoietic cells from the co-cultures were transplanted into sublethally irradiated NOD/SCID/IL-2 receptor$\gamma^{-/-}$ (NSG) mice. Of note, the co-culture conditions were not designed to expand the number of CD34$^+$ cells, as the cultures did not include growth factors (in contrast to all current *ex vivo* expansion protocols).

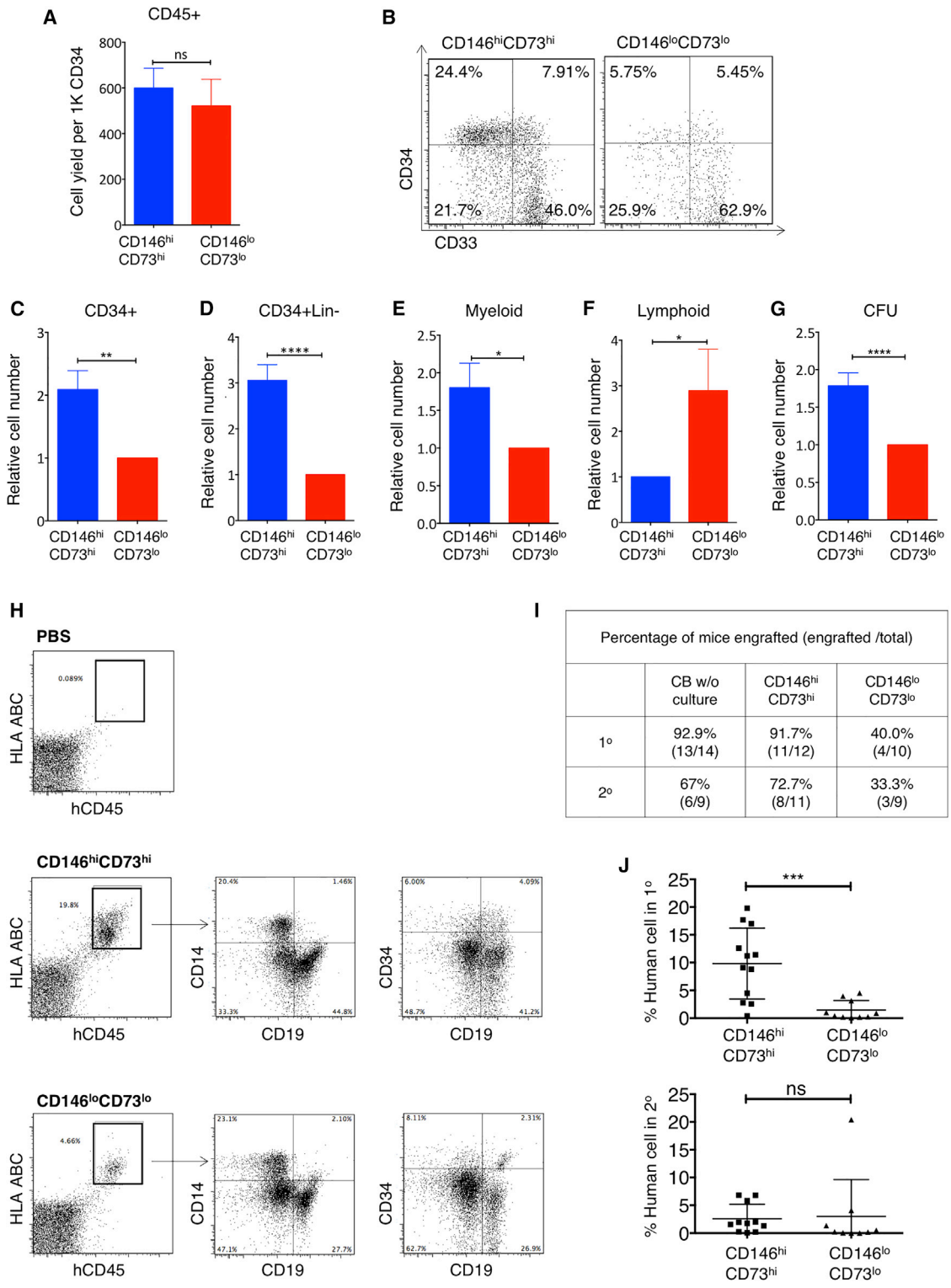

Figure 2. CD146^{hi}CD73^{hi} Mesenchyme Supports *Ex Vivo* Maintenance of Clonogenic, Engraftable, and Self-Renewing HSPCs

CD146^{hi}CD73^{hi} and CD146^{lo}CD73^{lo} mesenchymal cells generated from H1-derived hEMP were isolated and co-cultured as monolayers with CB CD34^{+} cells in 5% serum without added cytokines. After 2 weeks, hematopoietic cells were assayed (A–G) *in vitro* and (H–J) *in vivo*. (A) Total number of live (DAPI^{-}) CD45^{+} cells recovered from co-cultures, shown as cell yield normalized to 1,000 input CD34^{+} cells.

(legend continued on next page)

Based on flow cytometry analysis of bone marrow (Figure 2H), a similar frequency of mice transplanted with hematopoietic cells co-cultured with CD146^{hi}CD73^{hi} cells engrafted (albeit at lower levels) compared with those transplanted with fresh (non-cultured) CD34^{+} cells (11/12 versus 13/14, respectively) (Figures 2I and S3C), whereas only 40% of mice transplanted with hematopoietic cells from CD146^{lo}CD73^{lo} co-cultures demonstrated any detectable engraftment ($\geq$1% huCD45^{+}HLA^{+} cells in bone marrow) ($p < 0.01$) (Figure 2I). CD34^{+} progenitors and multi-lineage reconstitution (CD19^{+} lymphoid cells and CD14^{+} myeloid cells) were detected in the bone marrow, spleen, and peripheral blood of all mice that received hematopoietic cells from CD146^{hi}CD73^{hi} co-cultures (Figure 2H). Levels of engraftment were also significantly higher in animals that received CD146^{hi}CD73^{hi} co-cultures compared with CD146^{lo}CD73^{lo} co-cultures ($p < 0.001$) (Figure 2J). Irrespective of stromal co-culture conditions, mice that demonstrated primary engraftment could engraft in secondary recipients (Figure 2J).

Together, these data indicate that at least two functionally distinct mesenchymal populations were generated from hPSC-derived mesoderm; high CD146 and CD73 expression marked a mesenchymal subpopulation capable of maintaining engraftable HSPCs *ex vivo*, while CD146^{lo}CD73^{lo} mesenchyme had significantly less HSPC-supportive capacity.

HSPC Support Is Sustained through Intercellular Interactions, in Part by Notch Signaling

Prevention of direct contact between CD146^{hi}CD73^{hi} cells and CB CD34^{+} cells using a transwell culture system significantly reduced the number of CD34^{+}Lin^{-} cells maintained in culture ($p < 0.05$, $n = 3$) (Figure 3A). Output of CD146^{lo}CD73^{lo} co-cultures was also reduced in transwells, although to a lesser degree. Thus intercellular mechanisms provide at least part of the HSPC-supportive capacity of CD146^{hi}CD73^{hi} mesenchyme.

Notch signaling is a well-established cell contact-dependent paracrine factor and deletion of Jagged1 (encoded by *Jag1*) results in premature exhaustion of the murine HSC pool (Poulos et al., 2013). Both mesenchymal subsets expressed the Notch ligand *JAG1*, with significantly higher levels in CD146^{hi}CD73^{hi} mesenchyme (Figures 3B, S2A, and S2B); *DLL4* and *DLL1* were not expressed in either mesenchymal population (not shown). Expression of the Notch target *HES1* tended to be higher in the CD34^{+} cells co-cultured with CD146^{hi}CD73^{hi} mesenchyme compared with CD146^{lo}CD73^{lo} supported hematopoietic cells ($p = 0.1789$) (Figure 3C). Addition of a neutralizing antibody to human JAG1 caused a profound (>300-fold) decrease in the number of CD34^{+}Lin^{-} cells in CD146^{hi}CD73^{hi} co-cultures ($p \leq 0.05$, $n = 3$) and 250-fold decrease in CD146^{lo}CD73^{lo} co-cultures (Figure 3D). Of note, cell output was not significantly reduced when anti-JAG1 was added to co-cultures on OP9, a mouse stromal cell line, thus excluding non-specific cytotoxicity from the blocking antibody (Figure S4A).

Thus, although expression of JAG1 was significantly higher in CD146^{hi}CD73^{hi} stroma, HSPC support was dependent on JAG1-mediated activation of Notch signaling in both types of hPSC-mesenchymal co-cultures.

Wnt Inhibitors Are Highly Expressed in CD146^{hi}CD73^{hi} Stroma

Across the entire RNA-seq dataset, the most highly differentially expressed gene between CD146^{hi}CD73^{hi} and CD146^{lo}CD73^{lo} cells was the Wnt antagonist Secreted Frizzled-Related Protein 1 (*SFRP1*) (33-fold difference, FDR < 0.01) (Figure 3E). Expression of other Wnt inhibitors was also significantly higher in CD146^{hi}CD73^{hi} mesenchyme including *SFRP2* (FDR < 0.001) and *DKK1* (FDR < 0.001) (Figure 3E). Expression of Wnt downstream targets *TCF7* and *LEF1* was significantly higher in hematopoietic cells supported by CD146^{lo}CD73^{lo} co-cultures compared with those by CD146^{hi}CD73^{hi} mesenchyme ($n = 5$, $p < 0.05$) (Figure 3F).

Although neither addition of soluble SFRP1 or inhibition of SFRP1 had any detectable effect on HSPCs in either CD146^{hi}CD73^{hi} or CD146^{lo}CD73^{lo} co-cultures (Figure S4B), addition of a Wnt agonist, the GSK-3 inhibitor CHIR99021

(B) Representative FACS analysis of CD45^{+} gated cells from co-cultures.
(C–G) Cell yield of CD34^{+}, CD34^{+} Lin^{-}, CD14^{+} myeloid, CD10^{+}/CD19^{+} B lymphoid cells, and CFU (after re-plating) recovered from 2-week CD146^{hi}CD73^{hi} co-cultures, normalized to CD146^{lo}CD73^{lo} co-cultures.
(A and C–G) n = 16 independent experiments, each in duplicate. Shown are mean ± SEM. *p < 0.05, **p < 0.01, ****p < 0.0001; unpaired two-tailed Student's t test.
(H) Flow cytometry showing gating for the detection of human cells (hCD45^{+}HLA ABC^{+}) and multi-lineage reconstitution after primary transplant. PBS control with no cells injected.
(I) Proportion of mice with engraftment, i.e., detection of >1% human cells after primary transplant (1°) with 1 × 10^{5} CD45^{+} cells obtained either from fresh CB CD34^{+} cells (CB w/o culture), or 2 weeks after co-culture on CD146^{hi}CD73^{hi} or CD146^{lo}CD73^{lo}.
(J) Engraftment (percent of human cells) of mice 6 weeks after primary and secondary transplants (n = 5 independent experiments, total 9–14 mice per group; ***p <.0001; ns, not significant).
Error bars represent SEM. See also Figure S3.

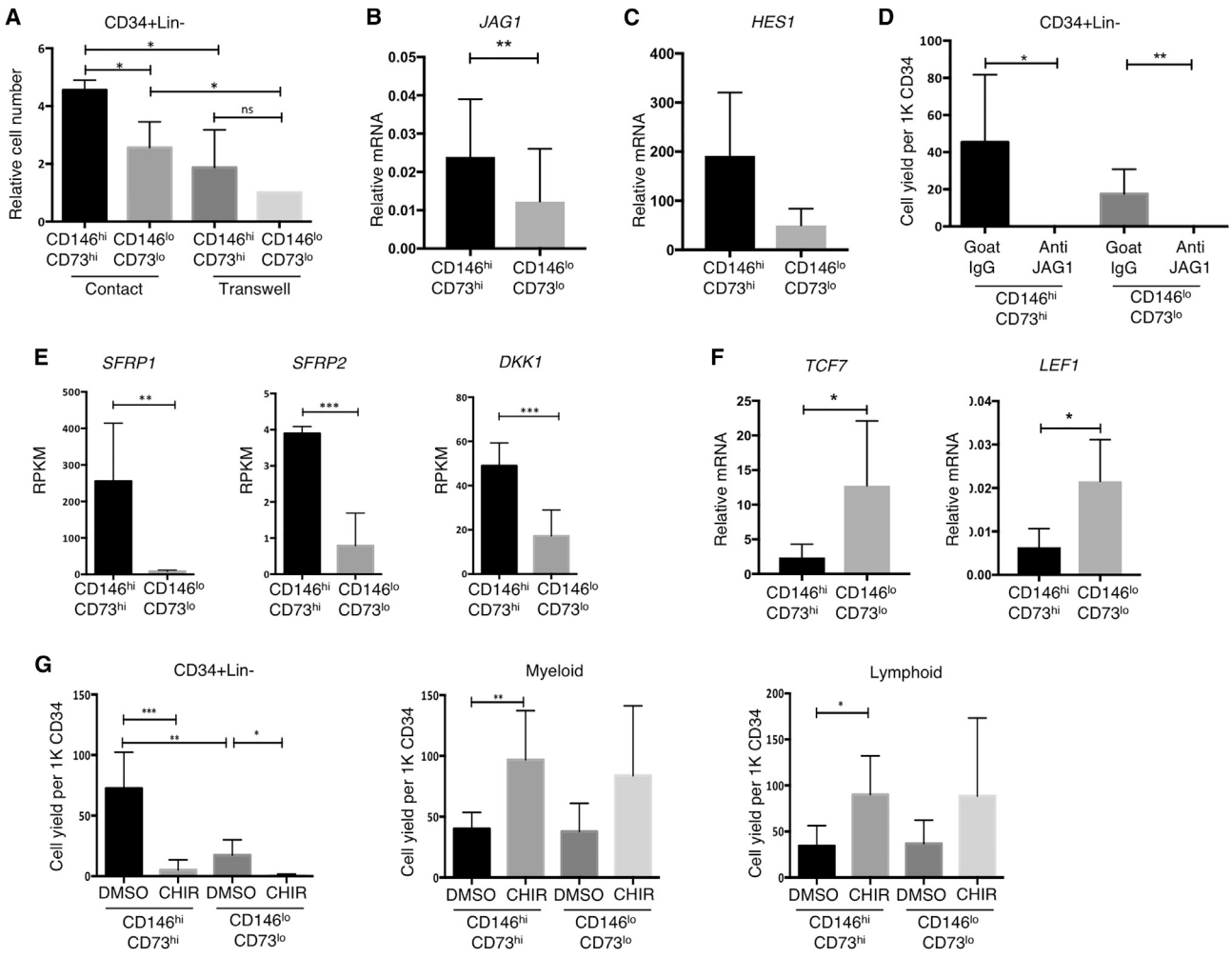

Figure 3. Notch Inhibition and Activation of Wnt Signaling in hPSC-Mesenchyme Co-cultures Leads to Loss of HSPC

(A) Shown is relative number of $CD34^{+}Lin^{-}$ cells in contact and transwell co-culture normalized to yield from $CD146^{lo}CD73^{lo}$ transwell co-cultures (n = 3 independent experiments, mean ± SEM. *p < 0.05).

(B) qRT-PCR of *JAG1* in $CD146^{hi}CD73^{hi}$ and $CD146^{lo}CD73^{lo}$ mesenchyme (n = 14 biological replicates, **p < 0.01).

(C) qRT-PCR of *HES1* in $CD34^{+}$ cells recovered from $CD146^{hi}CD73^{hi}$ and $CD146^{lo}CD73^{lo}$ mesenchyme after 7 days of co-culture without extra cytokines (n = 5 biological replicates, p = 0.1789).

(D) Number of $CD34^{+}$ Lin^{-} cells harvested from hPSC-mesenchyme after co-culture in the presence of human JAG1 blocking antibody or control goat IgG (*p < 0.05, **p < 0.01, n = 3 independent experiments).

(E) Expression of WNT inhibitors *SFRP1*, *SFRP2*, and *DKK1* in $CD146^{hi}CD73^{hi}$ and $CD146^{lo}CD73^{lo}$ mesenchyme (n = 3 biological replicates, RNA-seq **FDR < 0.01, ***FDR < 0.001).

(F) qRT-PCR of WNT target genes *TCF7* and *LEF1* in Lin^{+} cells recovered from $CD146^{hi}CD73^{hi}$ and $CD146^{lo}CD73^{lo}$ mesenchyme after 7 days of co-culture without extra cytokines (n = 5 biological replicates, *p < 0.05).

(G) $CD34^{+}$ Lin^{-}, myeloid and lymphoid cell numbers after activation of Wnt signaling by addition of 3 μM CHIR99021 (*p < 0.05, **p < 0.01, ***p < 0.001; ns, not significant; n = 3 independent experiments).

Error bars represent SEM. See also Figure S4.

(CHIR), promoted rapid differentiation into both myeloid and lymphoid lineages, and loss of $CD34^{+}Lin^{-}$ cells in both $CD146^{hi}CD73^{hi}$ and $CD146^{lo}CD73^{lo}$ co-cultures (Figure 3G). This latter observation is consistent with previous findings that canonical Wnt signaling regulates hematopoiesis in a dosage-dependent fashion, with high Wnt activation detrimental to HSC self-renewal leading to depletion of the LT-HSC pool (Famili et al., 2016; Luis et al., 2011). It is possible that functional redundancy among Wnt inhibitors obscures the impact of manipulating expression of single factors such as SFRP1 on HSPC support during co-culture.

hPSC-Derived CD146^{hi}CD73^{hi} Mesenchyme Shares a Coordinated Gene Expression Profile that Resembles that of Primary Human Pericytes

Given the complexity of signals produced in the HSC niche, it seems likely that no single factor or mechanism mediates the differential support of hematopoiesis from different mesenchymal subpopulations. As molecular characterization and functional studies of hPSC-derived CD146^{hi}CD73^{hi} and CD146^{lo}CD73^{lo} mesenchyme showed strong parallels to populations from primary human tissue, we performed comparative transcriptome analysis of each phenotypic population derived from hPSCs with those from primary adipose tissue (freshly isolated or after culture).

Principal-component analysis showed that the populations clustered mostly based on source rather than immunophenotype (data not shown). Similar observations that tissue-imprinted genes constitute major variances in unsupervised analysis have been reported in other comparative studies (Charbord et al., 2014). To uncover shared functional gene sets across stromal lines with HSPC-supportive capacity, we performed gene set enrichment analysis (Subramanian et al., 2005) as follows. The most up- and downregulated genes in hPSC-CD146^{hi}CD73^{hi} cells (compared with hPSC-CD146^{lo}CD73^{lo} cells) were defined as *positive* and *negative signatures*, respectively (FDR < 0.01 and at least 2-fold difference). These signatures of hPSC-derived CD146^{hi}CD73^{hi} cells were compared with the global expression profiles of primary CD146^{+} pericytes, ranked by differential expression to primary CD146^{-} cells. Significant enrichment was found between the positive signatures of hPSC-derived CD146^{hi}CD73^{hi} cells with genes upregulated in adult pericytes (Figure 4A, enrichment score of 1.36 and 1.78 in fresh and cultured pericytes respectively). Similarly, the negative signatures of hPSC-CD146^{hi}CD73^{hi} cells were significantly enriched in genes highly downregulated in primary pericytes (Figure 4B, enrichment score of −1.77 and −1.39). Thus hPSC- and adipose-derived CD146^{hi}CD73^{hi} cells exhibited similar transcriptional signatures.

The shared core transcriptional signature obtained from both hPSC- and adipose-derived CD146^{++} cells (104 genes, Table S1) was imported into the STRING database to identify known and predicted protein interactions (STRING protein-protein interaction enrichment $p < 10 \times 10^{-12}$) (Figure 4C). Of note, the dominant functional categories identified in the STRING analysis were those enriched in biological processes characteristic of pericytes, i.e., cell adhesion (FDR < 6×10^{-6}), vasculature development (FDR < 7×10^{-8}), regulation of cell motion (FDR < 3×10^{-8}), and wound healing (FDR < 3×10^{-4}), among others (Figure 4C). Therefore, the shared transcriptional signature between hPSC- and adipose-derived CD146^{++} cells is significantly enriched in processes involved in niche homeostasis and maintenance.

DISCUSSION

Mesenchymal stromal/stem cells, either derived from primary tissues or differentiated from hPSC, are conventionally isolated and expanded as a population of cells loosely defined by CD73, CD105, and CD90 expression (Murray et al., 2014). Our data strongly argue that phenotypically, molecularly, and functionally distinct populations coexist within these conventional definitions of mesenchymal stroma. Previously, CD146 was shown to define mesenchymal precursors adjacent to the vasculature of multiple human organs, including bone marrow and adipose tissues (Crisan et al., 2009). Other studies have derived CD146^{+} pericytes from hPSCs, demonstrating the capacity of these cells to reconstruct a vascular network (Dar et al., 2012; Kusuma et al., 2013; Orlova et al., 2014). Our previous work (Corselli et al., 2013) identified immunophenotypic subsets of mesenchyme isolated from human primary tissues and found that a subpopulation of perivascular mesenchyme with high expression of CD146 possessed significantly greater HSPC supporting ability. In the current paper, we show that two phenotypically, functionally, and molecularly distinct mesenchymal populations can be faithfully recapitulated in the hPSC system. We also provide the transcriptome profiling of these mesenchymal populations, revealing the HSPC-supportive CD146^{hi}CD73^{hi} cells to be closely related to primary pericytes.

hPSC-derived CD146^{hi}CD73^{hi} mesenchyme showed high expression of *NES*, *LEPR*, and *CSPG4*, markers of peri-sinusoidal and peri-arteriolar cells in the murine HSC niche (Ding et al., 2012; Kunisaki et al., 2013; Méndez-Ferrer et al., 2010; Zhou et al., 2014). The relevance of these perivascular cells has recently been addressed in the context of human hematopoiesis (Corselli et al., 2013; Pinho et al., 2013). PDGFRα/CD140a, which is a long-known marker for murine mesenchymal stromal cells (MSCs), was also reported on human fetal bone marrow MSCs capable of supporting HSPC expansion (Pinho et al., 2013). In contrast, later studies using adult human bone marrow reported that MSCs with hematopoiesis-supporting ability were highly enriched within the CD140a$^{lo/-}$ population but not in CD140a^{+} cells (Li et al., 2014). These conflicting results may be explained by reports of human mesenchymal stroma, including our own (Corselli et al., 2013), which suggest that CD140a expression is differentially regulated both developmentally and across tissue types. A recent report demonstrated that nestin^{+} mesenchyme in the

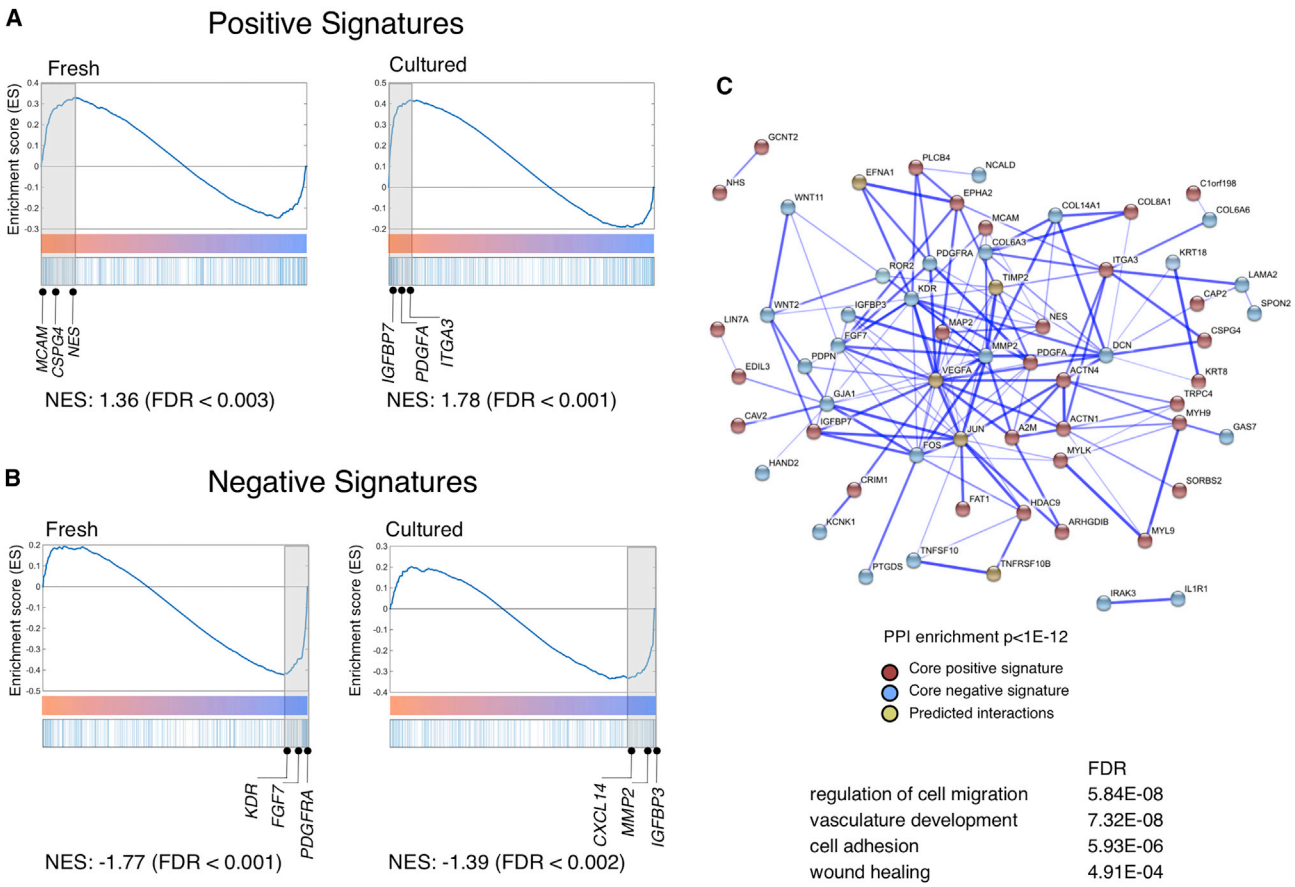

Figure 4. hPSC-Derived CD146^{hi}CD73^{hi} Mesenchyme Shares a Molecular Signature with Primary Human Adult Pericytes

(A and B) Gene set enrichment analysis of hPSC-derived mesenchyme and lipoaspirate-derived populations (both freshly sorted and cultured). (A) Positive and (B) negative signatures were defined, respectively, as up- and downregulated genes in hPSC-derived CD146^{hi}CD73^{hi} compared with hPSC-derived CD146^{lo}CD73^{lo} cells. The x axis represents genes ranked from positive to negative fold change in lipoaspirate-CD146^{+} compared with lipoaspirate-CD146^{-} cells. Genes in the core enrichment set are highlighted (shaded gray boxes) and selected genes in this core enrichment set are shown.

(C) Up- and downregulated genes common to the core sets of CD146^{hi} from hPSC and fresh and cultured primary CD146^{+} cells were imported into the STRING database, which identified a network of known protein-protein interactions (enrichment p value = 0), along with a number of high-confidence (score > 0.9999) predicted interactions. Line thickness is proportional to the confidence level of each interaction. See also Table S1.

murine fetal liver HSC niche expressed CD146 (Khan et al., 2016), further supporting the inclusion of CD146 in defining mesenchyme with HSC niche activity.

In the present study, both CD146^{hi}CD73^{hi} and CD146^{lo}CD73^{lo} cells from hPSCs expressed known HSC niche genes, such as *SLIT2* and *ANGPT1*. However, other niche factors, such as *KITL*, *JAG1*, and *IGFBP2*, were specifically upregulated in CD146^{hi}CD73^{hi} cells. As is likely for the components of the hematopoietic niche *in vivo*, we conclude the CD146^{hi}CD73^{hi} mesenchymal subset supports HSPCs through a combination of mechanisms that involve cell-cell contact (e.g., Notch signaling and adhesion molecules) and secreted factors (e.g., Wnt regulators and cytokines). Time course analysis for the development of CD146^{hi}CD73^{hi} and CD146^{lo}CD73^{lo} cells showed that they could each be distinguished early during mesenchymal differentiation. However, clonal data are needed to understand the developmental relationships of these cell types. It should also be acknowledged that it remains unclear whether the phenotypes examined in our study represent cell types at the extremes of a functional spectrum.

The identification of distinct mesenchymal subsets generated from hPSCs provides a foundation from which developmental and functional differences can be further defined, and the application of each population for cell therapy explored. The ability to prospectively isolate human stroma with HSC-supporting capacity is

particularly relevant given clinical interest in using stroma co-culture as a platform for HSC expansion (Hofmeister et al., 2007).

While this study focused on defining cellular subsets within hPSC-derived mesenchyme that would support a well-characterized HSPC population, the existence of distinct mesenchymal subsets during hPSC differentiation has broader implication for the directed differentiation of hPSCs toward definitive, functional HSCs. Further study will be needed to define the optimal hPSC-derived mesenchyme that would promote HSC specification.

EXPERIMENTAL PROCEDURES

Mesoderm Differentiation from hPSCs to Generate hEMPs

The hPSC lines H1 (WiCell, Madison, WI), and UCLA3 and UCLA6 (UCLA BSCRC hESC Core) were maintained and expanded on irradiated primary mouse embryonic fibroblasts (EMD Millipore, Billerica, MA). All hPSC experiments were approved by the UCLA Embryonic Stem Cell Research Oversight (ESCRO) committee. Mesoderm commitment was induced as described previously (Evseenko et al., 2010; Hoffman and Calvi, 2014) (Supplemental Experimental Procedures). $CD326^{-}CD56^{+}$ embryonic mesoderm progenitors (hEMPs) were isolated by flow cytometry at day 3.5 (Figure 1A) and seeded onto Matrigel for mesenchymal differentiation over the next 14 days.

Mesenchymal Differentiation from hEMPs

To induce mesenchymal differentiation, hEMPs were seeded at 50,000 cells/well into 6-well tissue culture plates, pre-coated with Matrigel. Day 0–7 of differentiation, MesenCult Proliferation Kit, Human (STEMCELL Technologies) supplemented with SB-431542 (10 μM, R&D Systems) was used. Day 0–3, 10 μM Rock inhibitor (Y27632 hydrochloride; R&D Systems) and 10 μg/mL gentamicin (Gibco, Thermo Fisher Scientific, Waltham, MA) were also added. Day 7–14, medium was switched to EGM-2 (Lonza) supplemented with SB-431542 (10 μM). Day 14–18, cells were dissociated into single-cell suspension with Accutase (Innovative Cell Technologies, San Diego, CA), and analyzed or isolated by fluorescence-activated cell sorting (FACS) (see Supplemental Experimental Procedures).

Co-culture of Stromal Cells and CB $CD34^{+}$ Cells

hEMP-derived mesenchyme ($CD146^{hi}CD73^{hi}$ and $CD146^{lo}CD73^{lo}$) was isolated from mesenchymal cultures after 14–18 days and re-plated in 96-well tissue culture-treated plates at 6.5×10^3 cells per well in 100 μL of EGM-2. Three days later, CB $CD34^{+}$ cells (>80% purity, 1×10^5 per well) were plated on 80% confluent stroma in 200 μL of co-culture medium consisting of RPMI 1640, L-glutamine, 5% fetal bovine serum, and penicillin/streptavidin. No supplemental cytokines were added unless otherwise indicated ($Lin^{-}CD34^{+}CD38^{-}$ experiments). Cells were harvested after 2 weeks unless otherwise indicated for FACS analysis, CFU assay, and *in vivo* repopulating assay.

Graphical and Statistical Analysis

Graphs were generated and statistics analyzed using GraphPad Prism software. Paired parametric two-tailed t tests were used to calculate p values except in cases where normalized values were used, in which case unpaired parametric t tests were used. $p < 0.05$ was considered statistically significant.

ACCESSION NUMBERS

The accession numbers for the RNA sequence data reported in this paper are GEO: GSE77879 and GSE83443.

SUPPLEMENTAL INFORMATION

Supplemental Information includes Supplemental Experimental Procedures, four figures, and one table and can be found with this article online at https://doi.org/10.1016/j.stemcr.2017.12.005.

AUTHOR CONTRIBUTIONS

C.J.C. and S.L., conception and design, collection and assembly of data, data analysis and interpretation, and manuscript writing. M.C., conception and design and collection of data. D.C., RNA-seq data analysis and interpretation. Y.Z. and C.B.H., collection of data. R.H. and B.P., RNA-seq data collection. G.M.C., conception and design, data analysis and interpretation, manuscript writing, financial support, and final approval of manuscript.

ACKNOWLEDGMENT

We thank J. Scholes and F. Codrea at the UCLA Broad Stem Cell Research Center (BSCRC) Flow Cytometry Core for assistance with cell sorting and R. Chan for assistance with specimen processing. The research was made possible by grants from the California Institute of Regenerative Medicine (CIRM), grant numbers RB3-05217 (to G.M.C.) and TR2-01821 (to B.P.). C.J.C. and M.C. acknowledge the support of the California Institute for Regenerative Medicine Training Grant (TG2-01169), and S.L. acknowledges the support of a fellowship grant from the UCLA BSCRC Training Program. Core services were supported by the Genomics Shared Resource (GSR) in the UCLA Jonsson Comprehensive Cancer Center (NIH/NCI 5P30CA016042), the BSCRC Flow Cytometry Core, and the UCLA Center for AIDS Research (CFAR) Virology Core Lab (NIH/NIAID AI028697).

Received: May 29, 2016
Revised: December 4, 2017
Accepted: December 5, 2017
Published: January 4, 2018

REFERENCES

Charbord, P., Pouget, C., Binder, H., Dumont, F., Stik, G., Levy, P., Allain, F., Marchal, C., Richter, J., Uzan, B., et al. (2014). A systems biology approach for defining the molecular framework of the hematopoietic stem cell niche. Cell Stem Cell *15*, 376–391.

Chin, C.J., Cooper, A.R., Lill, G.R., Evseenko, D., Zhu, Y., He, C.B., Casero, D., Pellegrini, M., Kohn, D.B., and Crooks, G.M. (2016). Genetic tagging during human mesoderm differentiation reveals

tripotent lateral plate mesodermal progenitors. Stem Cells *34*, 1239–1250.

Corselli, M., Chin, C.J., Parekh, C., Sahaghian, A., Wang, W., Ge, S., Evseenko, D., Wang, X., Montelatici, E., Lazzari, L., et al. (2013). Perivascular support of human hematopoietic stem/progenitor cells. Blood *121*, 2891–2901.

Crisan, M., Chen, C.W., Corselli, M., Andriolo, G., Lazzari, L., and Péault, B. (2009). Perivascular multipotent progenitor cells in human organs. Ann. N. Y. Acad. Sci. *1176*, 118–123.

Crisan, M., Yap, S., Casteilla, L., Chen, C.W., Corselli, M., Park, T.S., Andriolo, G., Sun, B., Zheng, B., Zhang, L., et al. (2008). A perivascular origin for mesenchymal stem cells in multiple human organs. Cell Stem Cell *3*, 301–313.

Dar, A., Domev, H., Ben-Yosef, O., Tzukerman, M., Zeevi-Levin, N., Novak, A., Germanguz, I., Amit, M., and Itskovitz-Eldor, J. (2012). Multipotent vasculogenic pericytes from human pluripotent stem cells promote recovery of murine ischemic limb. Circulation *125*, 87–99.

Ding, L., Saunders, T.L., Enikolopov, G., and Morrison, S.J. (2012). Endothelial and perivascular cells maintain haematopoietic stem cells. Nature *481*, 457–462.

Evseenko, D., Zhu, Y., Schenke-Layland, K., Kuo, J., Latour, B., Ge, S., Scholes, J., Dravid, G., Li, X., MacLellan, W.R., et al. (2010). Mapping the first stages of mesoderm commitment during differentiation of human embryonic stem cells. Proc. Natl. Acad. Sci. USA *107*, 13742–13747.

Famili, F., Brugman, M.H., Taskesen, E., Naber, B.E., Fodde, R., and Staal, F.J. (2016). High levels of canonical Wnt signaling lead to loss of stemness and increased differentiation in hematopoietic stem cells. Stem Cell Reports *6*, 652–659.

Ferrell, P.I., Hexum, M.K., Kopher, R.A., Lepley, M.A., Gussiaas, A., and Kaufman, D.S. (2014). Functional assessment of hematopoietic niche cells derived from human embryonic stem cells. Stem Cells Dev. *23*, 1355–1363.

Greenbaum, A., Hsu, Y.M., Day, R.B., Schuettpelz, L.G., Christopher, M.J., Borgerding, J.N., Nagasawa, T., and Link, D.C. (2013). CXCL12 in early mesenchymal progenitors is required for haematopoietic stem-cell maintenance. Nature *495*, 227–230.

Hoffman, C.M., and Calvi, L.M. (2014). Minireview: complexity of hematopoietic stem cell regulation in the bone marrow microenvironment. Mol. Endocrinol. *28*, 1592–1601.

Hofmeister, C.C., Zhang, J., Knight, K.L., Le, P., and Stiff, P.J. (2007). Ex vivo expansion of umbilical cord blood stem cells for transplantation: growing knowledge from the hematopoietic niche. Bone Marrow Transpl. *39*, 11–23.

Huynh, H., Iizuka, S., Kaba, M., Kirak, O., Zheng, J., Lodish, H.F., and Zhang, C.C. (2008). Insulin-like growth factor-binding protein 2 secreted by a tumorigenic cell line supports ex vivo expansion of mouse hematopoietic stem cells. Stem Cells *26*, 1628–1635.

Itkin, T., Gur-Cohen, S., Spencer, J.A., Schajnovitz, A., Ramasamy, S.K., Kusumbe, A.P., Ledergor, G., Jung, Y., Milo, I., Poulos, M.G., et al. (2016). Distinct bone marrow blood vessels differentially regulate haematopoiesis. Nature *532*, 323–328.

Khan, J.A., Mendelson, A., Kunisaki, Y., Birbrair, A., Kou, Y., Arnal-Estapé, A., Pinho, S., Ciero, P., Nakahara, F., Ma'ayan, A., et al. (2016). Fetal liver hematopoietic stem cell niches associate with portal vessels. Science *351*, 176–180.

Kobayashi, H., Butler, J.M., O'Donnell, R., Kobayashi, M., Ding, B.S., Bonner, B., Chiu, V.K., Nolan, D.J., Shido, K., Benjamin, L., et al. (2010). Angiocrine factors from Akt-activated endothelial cells balance self-renewal and differentiation of haematopoietic stem cells. Nat. Cell Biol. *12*, 1046–1056.

Kunisaki, Y., Bruns, I., Scheiermann, C., Ahmed, J., Pinho, S., Zhang, D., Mizoguchi, T., Wei, Q., Lucas, D., Ito, K., et al. (2013). Arteriolar niches maintain haematopoietic stem cell quiescence. Nature *502*, 637–643.

Kusuma, S., Shen, Y.I., Hanjaya-Putra, D., Mali, P., Cheng, L., and Gerecht, S. (2013). Self-organized vascular networks from human pluripotent stem cells in a synthetic matrix. Proc. Natl. Acad. Sci. USA *110*, 12601–12606.

Li, H., Ghazanfari, R., Zacharaki, D., Ditzel, N., Isern, J., Ekblom, M., Méndez-Ferrer, S., Kassem, M., and Scheding, S. (2014). Low/negative expression of PDGFR-α identifies the candidate primary mesenchymal stromal cells in adult human bone marrow. Stem Cell Reports *3*, 965–974.

Luis, T.C., Naber, B.A., Roozen, P.P., Brugman, M.H., de Haas, E.F., Ghazvini, M., Fibbe, W.E., van Dongen, J.J., Fodde, R., and Staal, F.J. (2011). Canonical wnt signaling regulates hematopoiesis in a dosage-dependent fashion. Cell Stem Cell *9*, 345–356.

Murray, I.R., West, C.C., Hardy, W.R., James, A.W., Park, T.S., Nguyen, A., Tawonsawatruk, T., Lazzari, L., Soo, C., and Péault, B. (2014). Natural history of mesenchymal stem cells, from vessel walls to culture vessels. Cell Mol. Life Sci. *71*, 1353–1374.

Méndez-Ferrer, S., Lucas, D., Battista, M., and Frenette, P.S. (2008). Haematopoietic stem cell release is regulated by circadian oscillations. Nature *452*, 442–447.

Méndez-Ferrer, S., Michurina, T.V., Ferraro, F., Mazloom, A.R., Macarthur, B.D., Lira, S.A., Scadden, D.T., Ma'ayan, A., Enikolopov, G.N., and Frenette, P.S. (2010). Mesenchymal and haematopoietic stem cells form a unique bone marrow niche. Nature *466*, 829–834.

Nakamura-Ishizu, A., Okuno, Y., Omatsu, Y., Okabe, K., Morimoto, J., Uede, T., Nagasawa, T., Suda, T., and Kubota, Y. (2012). Extracellular matrix protein tenascin-C is required in the bone marrow microenvironment primed for hematopoietic regeneration. Blood *119*, 5429–5437.

Orlova, V.V., Drabsch, Y., Freund, C., Petrus-Reurer, S., van den Hil, F.E., Muenthaisong, S., Dijke, P.T., and Mummery, C.L. (2014). Functionality of endothelial cells and pericytes from human pluripotent stem cells demonstrated in cultured vascular plexus and zebrafish xenografts. Arterioscler. Thromb. Vasc. Biol. *34*, 177–186.

Pinho, S., Lacombe, J., Hanoun, M., Mizoguchi, T., Bruns, I., Kunisaki, Y., and Frenette, P.S. (2013). PDGFRα and CD51 mark human nestin+ sphere-forming mesenchymal stem cells capable of hematopoietic progenitor cell expansion. J. Exp. Med. *210*, 1351–1367.

Poulos, M.G., Guo, P., Kofler, N.M., Pinho, S., Gutkin, M.C., Tikhonova, A., Aifantis, I., Frenette, P.S., Kitajewski, J., Rafii, S.,

et al. (2013). Endothelial Jagged-1 is necessary for homeostatic and regenerative hematopoiesis. Cell Rep. *4*, 1022–1034.

Sacchetti, B., Funari, A., Michienzi, S., Di Cesare, S., Piersanti, S., Saggio, I., Tagliafico, E., Ferrari, S., Robey, P.G., Riminucci, M., et al. (2007). Self-renewing osteoprogenitors in bone marrow sinusoids can organize a hematopoietic microenvironment. Cell *131*, 324–336.

Subramanian, A., Tamayo, P., Mootha, V.K., Mukherjee, S., Ebert, B.L., Gillette, M.A., Paulovich, A., Pomeroy, S.L., Golub, T.R., Lander, E.S., et al. (2005). Gene set enrichment analysis: a knowledge-based approach for interpreting genome-wide expression profiles. Proc. Natl. Acad. Sci. USA *102*, 15545–15550.

Vodyanik, M.A., Yu, J., Zhang, X., Tian, S., Stewart, R., Thomson, J.A., and Slukvin, I.I. (2010). A mesoderm-derived precursor for mesenchymal stem and endothelial cells. Cell Stem Cell *7*, 718–729.

Zhang, C.C., Kaba, M., Iizuka, S., Huynh, H., and Lodish, H.F. (2008). Angiopoietin-like 5 and IGFBP2 stimulate ex vivo expansion of human cord blood hematopoietic stem cells as assayed by NOD/SCID transplantation. Blood *111*, 3415–3423.

Zhou, B.O., Yue, R., Murphy, M.M., Peyer, J.G., and Morrison, S.J. (2014). Leptin-receptor-expressing mesenchymal stromal cells represent the main source of bone formed by adult bone marrow. Cell Stem Cell *15*, 154–168.